

## Ab initio Studies on Acene Tetramers: Herringbone Structure

Young Hee Park, Kiyull Yang,<sup>†,\*</sup> Yun-Hi Kim, and Soon Ki Kwon<sup>‡</sup>

Department of Chemistry, <sup>†</sup>Department of Chemistry Education, <sup>‡</sup>School of Nano & Advanced Materials and Engineering Research Institute, Gyeongsang National University, Jinju 660-701, Korea. \*E-mail: kyang@gsnu.ac.kr

Received June 14, 2007

The structures, energetics and transfer integrals of the acene tetramers up to pentacene are investigated with the *ab initio* molecular orbital method at the level of second-order Møller-Plesset perturbation theory (MP2). Calculated geometries for the herringbone-style structures found in the crystal structure were characterized as local minima, however the geometrical discrepancy between crystal and MP2 theoretical structure is reasonably small. The binding energy of pentacene tetramer was calculated up to 40 kcal/mol (MP2/6-31G(d)) and about 90 kcal/mol (MP2/aug-cc-pVDZ), and the latter seems to be too much overestimated. The tendency of the hole transfer integrals computed with *ab initio* MP2/3-21G(d) geometry is well agreement with those estimated with crystal structure with some discrepancy, and the gradual increment of the transfer integrals at the crystal geometry is attributed to mainly packing structure rather than the intrinsic property of acene such as a size of acene.

**Key Words** : Organic thin-film transistor (OTFT), Hole/electron transfer rate,  $\pi$ - $\pi$  interaction, Transfer integral, Binding energy of acene tetramer

### Introduction

The understanding of weak interactions between  $\pi$  systems was of great interest in both many fundamental chemical point of view and applications in the field of electronics and opto-electronics. Among the recent applications, the designing of new novel organic thin-film transistor (OTFT) as a switching device for the flexible display panel has attracted much interest.<sup>1-5</sup> Several aromatic compounds such as oligoacenes and oligothiophenes have been studied extensively due to the remarkable electronic properties including conductivity.<sup>6-8</sup> As a good OTFT material, high charge-carrier mobility is one of the important factors in designing a novel material. The measured hole and electron mobilities of oligoacene crystals show a band hopping transition occurring at about room temperature: there are two different regimes, band-like mechanism at low temperature, and hopping mechanism at high temperature.

A hopping of hole or electron can be described as an electron transfer (ET) reaction from a charged, relaxed unit to an adjacent neutral unit, and the mobility depends on the electron transfer rate. At high temperature, the ET or hopping rate are given by eq. (1), according to the semi-classical Marcus theory.<sup>9,10</sup>

$$k_{\text{ET}} = \frac{4\pi^2}{h} \frac{1}{\sqrt{4\pi\lambda k_B T}} t^2 \cdot \exp\left(-\frac{\lambda}{4k_B T}\right) \quad (1)$$

The reorganization energy,  $\lambda$  measures the strength of hole (electron)-vibration interaction, which needs to be small for efficient transport. The absolute value of the transfer integral for hole or electron transfer can be estimated from the energy difference,  $2t = (\epsilon_{\text{HOMO(LUMO)+1}} - \epsilon_{\text{HOMO(LUMO)}})$ , at a dimeric unit, and the larger the bandwidth

(the magnitude of transfer integral), the higher the hole (electron) mobility. Interchain transfer integral strongly depends on the geometrical arrangement of monomer units in single crystal or molecular cluster<sup>11</sup> while the intramolecular reorganization energy is purely intrinsic property of single molecule. Therefore it is quite valuable to examine the oligomeric structure of designed OTFT material to estimate transfer integrals prior to the synthesis and fabrication of the device. Consequently, this prompted us to determine geometry and binding energy of oligoacene tetramers theoretically by using *ab initio* molecular orbital theory, since the tetramer unit can be regarded as a repeating motif in the solid state.

Although there are many computational dimeric, trimeric or tetrameric structures for the oligoacenes such as benzene and naphthalene,<sup>12-18</sup> but few computational studies have been reported for the tetrameric structures for the oligoacenes because of the computational difficulty with quantum chemical methods. Hobza *et al.* reported structures and binding energies of benzene trimers and tetramers using nonempirical model (NEMO) potential calibrated from the coupled cluster calculations (CCSD) of benzene dimer.<sup>17</sup> They reported that binding energies of benzene tetramers lie in a range of  $-7.32 \sim -8.55$  kcal/mol for the relatively stable structures with a fourfold three-dimensional cyclic structure as a global minimum. Recently, Sherrill reported the binding energy of benzene tetramer as a range of  $-7.05 \sim -8.94$  kcal/mol at the MP2/cc-pVDZ+ level of theory.<sup>18</sup>

However, most theoretical studies in this field are focused on the origin of interactions, absolute binding energy and structures in the gas phase. Structural analysis of known OTFT materials, such as a pentacene has shown that the crystal structure of all these molecules shows the 'herringbone' (H) style depicted in Figure 1, where we only depicted

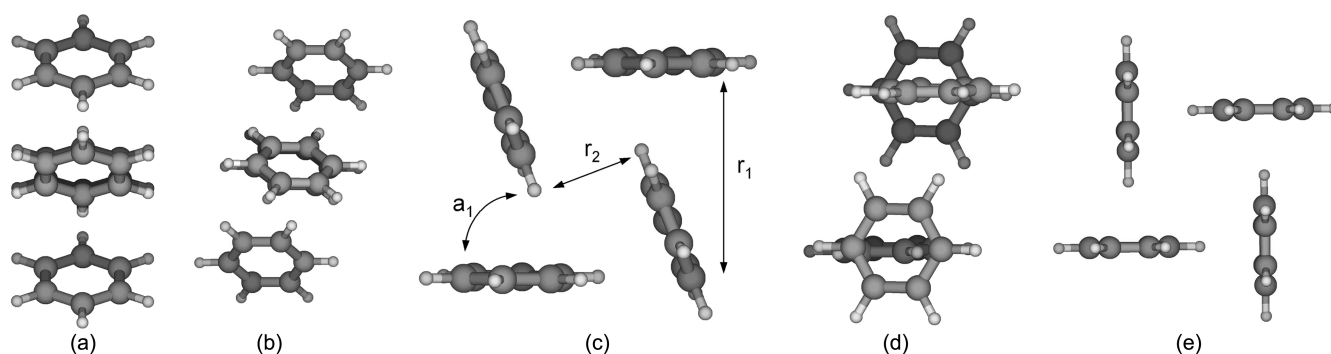


**Figure 1.** MP2 optimized structures of benzene tetramer motif. (a) herringbone structure (H); (b) slipped herringbone (S-H); (c) side view of (a) and (b); (d) slipped T-shape (S-T) structure; (e) side view of (d). Only slipped herringbone (S-H) and T-shape structures are found in solid state. All other acene tetramers in these calculations are performed for the configurations (a) and (b).

benzene tetramer for the clarity, and many oligoacenes and other oligomers show such a herringbone style, too.<sup>19</sup> The real herringbone structure found in solid state shows slipped structure in order to have the favorable  $\pi$ - $\pi$  interactions between the adjacent herringbone motifs. Hereafter, we term this herringbone style as a slipped herringbone (S-H), and the other, which can be regarded as a single motif in the absence of the adjacent herringbone motifs, as a herringbone (H) as depicted in Figure 1.

In this work we examine the herringbone structures and the binding energies of acene tetramers using *ab initio* method, since *ab initio* calculations of some of large structures have not been reported yet as far as we know.

Though the density functional theory (DFT) is a successful theoretical method in elucidating the structure-reactivity relationship in many organic and inorganic reactions with electron correlation, it still has a drawback for the demonstration of weak  $\pi$ - $\pi$  interaction even in a simple benzene dimer.<sup>12,20</sup> It is well known that the use of second-order Møller-Plesset perturbation theory (MP2), at least, is essential to predict geometries and proper binding energies of those clusters, even though attractive interaction is overestimated compared to the coupled cluster calculations (CCSD).<sup>21</sup> We choose MP2 method to examine the geometry and related properties and the range of binding energy of the acene tetramers in this work, because the CCSD method is computationally not feasible for the larger molecules.

### Computational Method

The Gaussian 03 program<sup>22</sup> was used for the *ab initio* molecular orbital calculation to compute structures and the binding energies. The basis sets employed in this work are 3-21G(d) for geometry optimization, and 6-31G(d), and aug-cc-pVDZ basis sets on carbon atom and cc-pVDZ basis sets on hydrogen for the computation of binding energies with MP2 correlation.<sup>23</sup> Although the MP2/3-21G(d) basis sets is a lower level of theory in these days, larger basis set and highly correlated method are not applicable for the computation of oligomers of OTFT materials as well as the pentacene molecule. Two kinds of initial geometries are

considered, *i.e.*, herringbone style (H) and slipped herringbone style (S-H) found in the solid state. For the benzene tetramers, we also calculate T-shape (T) and slipped T-shape (S-T) structures that were also found in the crystal structures. All degrees of freedom were fully relaxed in the geometry optimization with MP2/3-21G(d), and the binding energies of tetramers were computed through the single point calculations using larger basis sets. The basis set superposition error (BSSE) was calculated using the counterpoise method of Boys and Bernardi.<sup>24</sup> The hole transfer integrals for the dimeric unit at the computed geometries were calculated by semi-empirical ZINDO method to compare with the values reported by Brédas and co-workers.<sup>25</sup> All the computations were performed using one node (32 CPUs) of the IBM p690 supercomputer at the Korea Institute of Science and Technology Information (KISTI).

### Results and Discussion

The geometries of benzene tetramers were determined for H-type and T-shape, which are non-slipped structures with a proper symmetry restriction. Crystal structures termed as slipped herringbone (S-H) and slipped T-shape (S-T) were also optimized as local minima. The geometries of the rest of the oligoacenes are optimized by same manner with symmetry restriction. Some intermolecular geometric parameters between the acene units are summarized in Table 1 with the

**Table 1.** Geometries of crystal and optimized structures [MP2/3-21G(d)] for acene tetramer with S-H configuration. Distances between the monomeric units,  $r_1$  and  $r_2$ , are in angstrom and tilt angles,  $a_1$  are in degrees

	geometry	benzene	naphthalene	anthracene	tetracene	pentacene
$r_1$	crystal	6.3	6.2	6.8	6.9	6.7
	MP2	5.9	6.3	6.2	6.2	6.1
$r_2$	crystal	2.6	2.2	2.5	2.6	2.6
	MP2	3.1	2.6	2.7	2.7	2.8
$a_1$	crystal	57	52	50	51	52
	MP2	69	55	56	57	59

<sup>a</sup>Crystal structures of benzene,<sup>26</sup> naphthalene,<sup>27</sup> anthracene,<sup>28</sup> tetracene,<sup>29</sup> and pentacene,<sup>29</sup> are taken from Cambridge database.

**Table 2.** Binding energies (BE), BSSE and BSSE-corrected BE ( $BE_{\text{bsse}}$ ) of acene tetramers calculated by MP2/6-31G(d)/MP2/3-21G(d) and MP2/aug-cc-pVDZ//MP2/3-21G(d). Energies in kcal/mol

Structure (symmetry)	MP2/6-31G (d)			MP2/aug-cc-pVDZ			
	-BE	BSSE	$-BE_{\text{bsse}}$	-BE	BSSE	$-BE_{\text{bsse}}$	
benzene	H( $C_{2h}$ )	14.90	10.54	4.36	25.74	11.28	14.46
	S-H( $C_i$ )	15.01	10.26	4.75	25.43	11.02	14.41
	T( $C_{2h}$ )	14.78	10.22	4.56	24.07	10.74	13.33
	S-T( $C_i$ )	14.76	9.50	5.26	24.23	10.48	13.75
naphthalene	H( $C_{2h}$ )	30.75	19.80	10.95	54.82	24.64	30.18
	S-H( $C_i$ )	30.25	18.50	11.75	52.97	22.84	30.13
anthracene	H( $C_{2h}$ )	49.32	29.26	20.06	87.20	37.94	49.26
	S-H( $C_i$ )	45.99	26.80	19.19	83.05	35.12	47.93
tetracene	H( $C_{2h}$ )	69.21	39.70	29.51			66-71 <sup>a</sup>
	S-H( $C_i$ )	66.03	37.56	28.47			65-67 <sup>a</sup>
pentacene	H( $C_{2h}$ )	90.34	50.20	40.14			83-96 <sup>a</sup>
	S-H( $C_i$ )	87.91	48.26	39.65			81-89 <sup>a</sup>

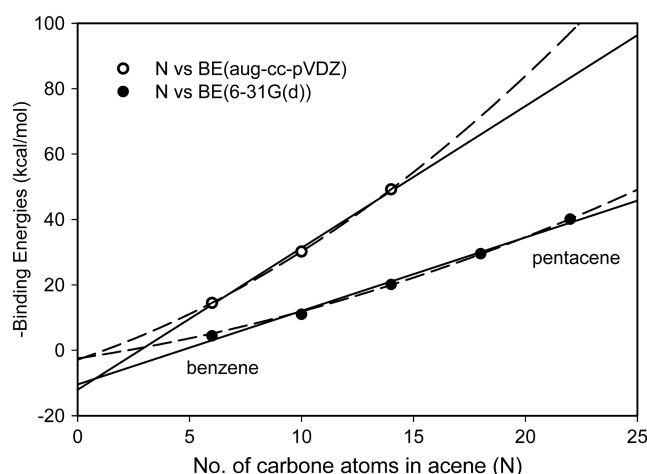
<sup>a</sup>Extrapolated. The lower and upper limits correspond to the linear and quadratic extrapolations, respectively.

experimental values.

Computed long-range cofacial distance  $r_1$  is smaller than that of the crystal structure and tilted angle between adjacent units is slightly larger than that of the crystal structure. However, the short-range cofacial distance  $r_2$  is almost same as that in the crystal structure. It is noteworthy that important geometric variable  $r_2$  which may affect the hole transfer integrals is very close to that in the crystal structure for the acenes larger than anthracene. The shorter distance  $r_1$  seems to reflect the strong long-range interaction at the MP2 method as mentioned above. In the crystal structure slipped tetramer motif can overlap to the adjacent motif along the  $c$ -axis in order to have the favorable energetics of the  $\pi$ - $\pi$  interactions.

Binding energies (BE) calculated at the MP2/6-31G(d)//MP2/3-21G(d) and MP2/aug-cc-pVDZ//MP2/3-21G(d) are summarized in Table 2.  $BE_{\text{bsse}}$  is binding energy corrected for the basis set superposition error (BSSE). During the computation of larger molecules at the level of MP2/aug-cc-pVDZ, we encountered computational difficulties in storing the huge amount of two electron integrals: the total numbers of basis functions at this level are 1896 and 2300, for tetracene tetramer and pentacene tetramer, respectively. Therefore, BE of tetracene and pentacene at this level were estimated by extrapolation, since there are apparently linear and/or quadratic relationships between the BE and the number of carbon atoms (N) in the acenes as shown in Figure 2.

Generally  $BE_{\text{bsse}}$  obtained with a larger basis set (aug-cc-pVDZ) are considerably larger than those obtained with 6-31G(d). In the absence of relevant experimental binding energies of larger acene tetramers, one cannot rationalize the proper binding energy of tetramers. However, experimental gas-phase binding energy ( $-12.11$  kcal/mol) for the naphtha-

**Figure 2.** Linear (solid line) and quadratic (dashed line) relationships between number of carbon atoms in acene (N) and binding energies (BE).

lene tetramer reported by Fujiwara *et al.*<sup>30</sup> encourages us to believe that the binding energy of  $-11.75$  kcal/mol for the tetramer at the MP2/6-31G(d) seems to be quite reasonable. Though the binding energy of benzene tetramer calculated by the MP2/6-31G(d) is lower than the reported theoretical range of  $-7 \sim -9$  kcal/mol, such a lower binding energy is not too bad considering the fact that the theoretical binding energy of the range of  $-2.2 \sim -4.73$  kcal/mol is always lower than the well-known experimental binding energy of  $-1.6$  kcal/mol for the benzene dimer.<sup>31</sup> The binding energy obtained at the MP2 with lower basis sets such as a 6-31G(d) may result from the cancellation of errors as pointed out by Sherrill and co-workers<sup>18</sup>: 'small basis sets underestimate binding while MP2 overestimates binding'. The binding energies of H are larger than those of S-H, but these differences will be overcome by interactions with the adjacent motifs in the crystal structure. It is interesting to note that the BEs calculated (or estimated) with a larger basis set (MP2/aug-cc-pVDZ) are considerably overestimated in the tetramer, though the BE of benzene dimer calculated using the

**Table 3.** Hole transfer integrals (eV) estimated using ZINDO//MP2/3-21G(d) method

structure	Direction	benzene	naphthalene	anthracene	tetracene	pentacene
S-H	a	0.079	0.111	0.216	0.157	0.199
	b	0.0008	0.000	0.0003	0.0003	0.0005
	d <sub>1</sub>	0.093	0.143	0.187	0.368	0.361
	d <sub>2</sub>	n/a	n/a	n/a	0.197	0.334
	2t <sup>a</sup>	0.093	0.143	0.216	0.368	0.361
H	a	0.090	0.180	0.222	0.229	0.246
	b	0.0005	0.0008	0.0008	0.0008	0.0008
	d <sub>1</sub>	0.130	0.338	0.337	0.316	0.335
	2t <sup>a</sup>	0.130	0.338	0.337	0.316	0.335
solid state <sup>b</sup>	2t		0.077	0.097	0.138	0.196

<sup>a</sup>The largest values in any directions. <sup>b</sup>Reference 25.

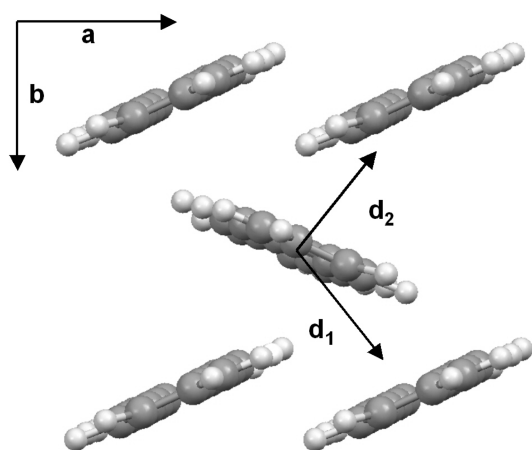


**Figure 3.** Illustration of crystal packing directions.  $d_1$  and  $d_2$  refer to the inequivalent directions.

same basis set is slightly overestimated than those obtained by complete basis sets (CBS) with CCSD(T).<sup>13</sup>

We calculated the hole transfer integrals for the dimeric unit by semi-empirical ZINDO method at the optimized geometries of the MP2/3-21G(d), and the results are summarized in Table 3, and appropriate axes are depicted in Figure 3.

The integrals increased from benzene to pentacene, even though there is a slight irregularity beyond anthracene. Furthermore, the magnitudes of integrals are larger than those obtained using solid state geometries,<sup>25,32</sup> and the integrals are almost constant at the geometry of non-slipped herringbone (H) structures except benzene. To find out the discrepancy in transfer integrals between the calculated and solid-state geometries, we calculated the integrals of anthracene, tetracene, and pentacene using the intermolecular geometries of pentacene tetramer. The calculated hole transfer integrals,  $2t$ , were plotted as a function of displacement ( $D$ ) as shown Figure 4.

Astonishingly, hole transfer integrals (HOMO bandwidth) are almost constant with the value of 0.2 eV regardless of the size of acenes at zero displacement ( $D = 0$ ), and the integrals are gradually decreased with oscillation as displacement increased as usual. The constant HOMO bandwidth at  $D = 0$ , regardless of the size of acene, can be rationalized by examining the shape of HOMO or HOMO-1 orbitals. The

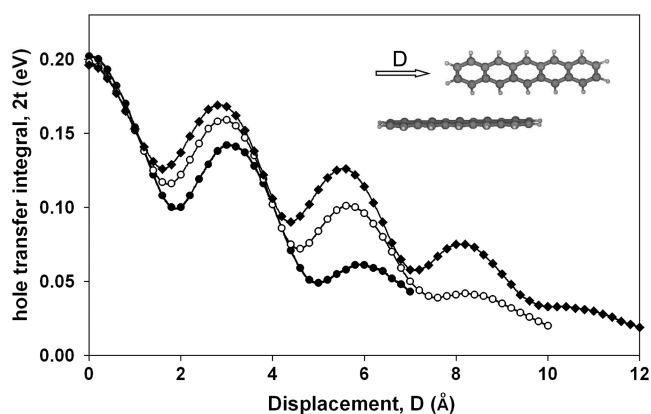


**Figure 4.** Evolution of ZINDO-calculated electronic splitting of the HOMO levels in a dimer formed by two anthracene (●), tetracene (○) and pentacene (◆) units as a function of displacement. Intermolecular geometries of acenes are taken from those of the pentacene tetramer.

HOMO-1 orbitals, which are positive combination of two  $\pi$  molecular orbitals of monomeric units, are illustrated in Figure 5 with equal contour value of 0.03. Very interestingly, distributions of wave function of each moiety in HOMO-1 (or HOMO) are not equal at larger acenes; wave functions in lower moiety are evenly distributed while those in upper moiety are accumulated at central two and three phenyl units, for tetracene and pentacene, respectively. Thus the overall overlap between the  $\pi$  orbitals of two acene units are almost the same, and this leads to the constant HOMO bandwidth at  $D = 0$ .

Therefore, the gradual increment (better hole transport) of the transfer integrals of the series of acenes in the crystal structure is mainly attributed to the crystal configuration in nature rather than the size of acenes.

## Conclusions

In order to propose a theoretical benchmarking in designing effective and useful materials for electronics and optoelectronics, we have performed *ab initio* molecular orbital calculations on acene tetramers. The herringbone structures of acene tetramer motif obtained at the MP2/3-21G(d) level of theory are in reasonable good agreement with those of crystal structure. In the absence of experimental binding

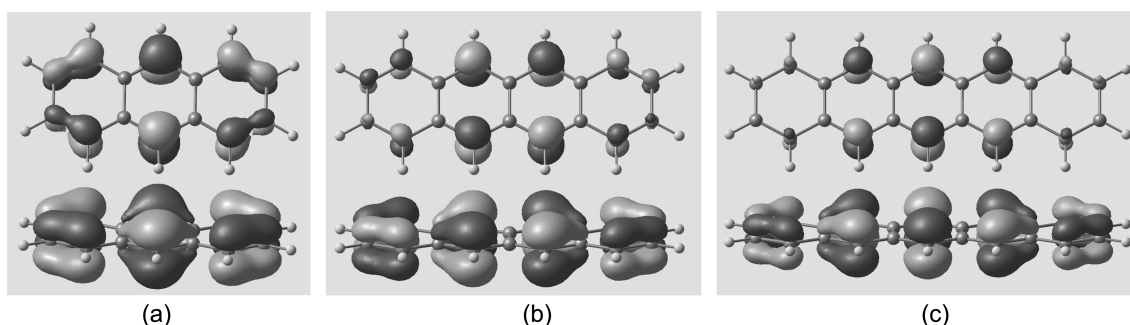


**Figure 5.** 3D contour plot of HOMO-1 wave function of anthracene (a), tetracene (b) and pentacene (c) dimeric units.

energy for larger acene tetramers, binding energy calculated at the MP2/6-31G(d) level of theory seems to be better than that calculated at the MP2/aug-cc-pVDZ level of theory. The tendency of hole transfer integrals estimated with the MP2/3-21G(d) geometries agrees well with those obtained with crystal structure, though there is a discrepancy at the absolute value. Well-behaved gradual increment of transfer integrals from naphthalene to pentacene, which is estimated using the crystal structure, is attributed to mainly crystal packing rather than the intrinsic property of acene such as the size of acene. Based on these results, computer-aided molecular design using the geometry obtained at the MP2/3-21G(d) for the larger cluster molecules, especially for the  $\pi$ - $\pi$  stacked clusters, can be used to predict physicochemical parameters of materials and this information can be useful in screening most desirable structures before synthesis.

**Acknowledgments.** The authors wish to thank for the financial support from the Ministry of Commerce, Industry and Energy of Korea through the 21C Frontier program (F0004021-2007-23). The authors also would like to acknowledge the support from Korea Institute of Science and Technology Information under 'Grand Challenge Support Program', and the use of the computing system of the Supercomputing Center is also greatly appreciated. K. Yang also thanks for the support of Chemistry Fund, Gyeongsang National University, and thanks for the helpful discussions of Dr. O. Kwon at Samsung Advanced Institute of Technology (SAIT).

### References

- Merlo, J. A.; Newman, C. R.; Gerlach, C. P.; Kelly, T. W.; Muryres, D. V.; Fritz, S. E.; Toney, M. F.; Frisbie, C. D. *J. Am. Chem. Soc.* **2005**, *127*, 3997.
- Chen, F.-C.; Chu, C.-W.; He, C.; Yang, Y. *Appl. Phys. Lett.* **2004**, *85*, 3295.
- Reese, C.; Roberts, M.; Ling, M. M.; Bao, Z. *Mater. Today* **2004**, *7*, 20.
- Brédas, J.-L.; Beljonne, D.; Coropceanu, V.; Cornil, J. *Chem. Rev.* **2004**, *104*, 4971.
- Cornil, J.; Calbert, J.-P.; Beljonne, D.; Silbey, R.; Brédas, J.-L. *Adv. Mater.* **2000**, *12*, 978.
- Sheraw, C. D.; Zhou, L.; Huang, J. R.; Gundlach, D. J.; Jackson, T. N.; Kane, M. G.; Hill, I. G.; Hammond, M. S.; Campi, J.; Greening, B. K.; Francl, J.; West, J. *Appl. Phys. Lett.* **2002**, *80*, 1088.
- Dimitrakopoulos, C. D.; Purushothaman, S.; Kymissis, J.; Callegari, A.; Shaw, J. M. *Science* **1999**, *283*, 822.
- Garnier, F.; Hajlaoui, R.; Yassar, A.; Srivastata, P. *Science* **1994**, *265*, 1684.
- Marcus, R. A. *Rev. Mod. Phys.* **1993**, *65*, 599.
- Bixon, M.; Jortiner, J. *Electron Transfer: From Isolated Molecules to Biomolecules*, *Adv. Chem. Phys.* 106-107; Wiley: New York, 1999.
- Brédas, J.-L.; Calbert, J. P.; da Silva Filho, D. A.; Cornil, J. *Proc. Natl. Acad. Sci. USA* **2002**, *99*, 5804.
- Sinnokrot, M. O.; Sherrill, C. D. *J. Phys. Chem. A* **2006**, *110*, 10656.
- Sinnokrot, M. O.; Valeev, E. F.; Sherrill, C. D. *J. Am. Chem. Soc.* **2002**, *124*, 10887.
- Gonzales, C.; Lim, E. C. *J. Phys. Chem. A* **2001**, *105*, 1904.
- Walsh, T. R. *Chem. Phys. Lett.* **2002**, *363*, 45.
- Gonzales, C.; Lim, E. C. *J. Phys. Chem. A* **2001**, *105*, 1904.
- Engkvist, O.; Hobza, P.; Selzle, H. L.; Schlag, E. W. *J. Chem. Phys.* **1999**, *110*, 5758.
- Tauer, T. P.; Sherrill, C. D. *J. Phys. Chem. A* **2005**, *109*, 10475.
- Curtis, M. D.; Cao, J.; Kampf, J. W. *J. Am. Chem. Soc.* **2004**, *126*, 4318.
- Johnson, E. R.; Wolkow, R. A.; Dilabio, G. A. *Chem. Phys. Lett.* **2004**, *394*, 334.
- Raghavachari, K.; Trucks, G. W.; Pople, J. A.; Head-Gordon, M. *Chem. Phys. Lett.* **1989**, *157*, 479.
- Frisch, M. J.; Trucks, G. W.; Schlegel, H. B.; Scuseria, G. E.; Robb, M. A.; Cheeseman, J. R.; Zakrzewski, V. G.; Montgomery, J. A., Jr.; Stratmann, R. E.; Burant, J. C.; Dapprich, S.; Millam, J. M.; Daniels, A. D.; Kudin, K. N.; Strain, M. C.; Farkas, O.; Tomasi, J.; Barone, V.; Cossi, M.; Cammi, R.; Mennucci, B.; Pomelli, C.; Adamo, C.; Clifford, S.; Ochterski, J.; Petersson, G. A.; Ayala, P. Y.; Cui, Q.; Morokuma, K.; Malick, D. K.; Rabuck, A. D.; Raghavachari, K.; Foresman, J. B.; Cioslowski, J.; Ortiz, J. V.; Baboul, A. G.; Stefanov, B. B.; Liu, G.; Liashenko, A.; Piskorz, P.; Komaromi, I.; Gomperts, R.; Martin, R. L.; Fox, D. J.; Keith, T.; Al-Laham, M. A.; Peng, C. Y.; Nanayakkara, A.; Gonzalez, C.; Challacombe, M.; Gill, P. M. W.; Johnson, B. G.; Chen, W.; Wong, M. W.; Andres, J. L.; Head-Gordon, M.; Replogle, E. S.; Pople, J. A. *Gaussian: Pittsburgh, PA*, 2003.
- Dunning, T. H. *J. Chem. Phys.* **1989**, *90*, 1007.
- Boys, S. F.; Bernardi, F. *Mol. Phys.* **1970**, *19*, 553.
- Cheng, Y. C.; Silbey, R. J.; da Silva Filho, D. A.; Calbert, J. P.; Cornil, J.; Brédas, J.-L. *J. Chem. Phys.* **2003**, *118*, 3764.
- Lommerse, J. P.; Motherwell, W. D.; Ammon, H. L.; Dunitz, J. D.; Gavezzotti, A.; Hofmann, D. W.; Leusen, F. J.; Mooij, W. T.; Price, S. L.; Schweizer, B.; Schmidt, M. U.; van Eijck, B. P.; Verwer, P.; Williams, D. E. *Acta Crystallogr. Sect B: Struct. Sci.* **2000**, *56*, 697.
- Ponomarev, V. I.; Filipenko, O. S.; Atovmyan, L. O. *Kristallografiya* **1976**, *21*, 392.
- Brock, C. P.; Dunitz, J. D. *Acta Crystallogr. Sect B: Struct. Sci.* **1990**, *46*, 795.
- Holmes, D.; Kumaraswamy, S.; Matzger, A. J.; Vollhardt, K. P. C. *Chem-Eur. J.* **1999**, *5*, 3399.
- Fujiwara, T.; Lim, E. C. *J. Phys. Chem. A* **2003**, *107*, 4381.
- Krause, H.; Ermstberger, B.; Neusser, H. J. *Chem. Phys. Lett.* **1991**, *184*, 411.
- Cornil, J.; Calbert, J. Ph.; Brédas, J.-L. *J. Am. Chem. Soc.* **2001**, *123*, 1250.